Quantum circuit analog of the dynamical Casimir effect

Toshiyuki Fujii,[1,2,*] Shigemasa Matsuo,[1,2] Noriyuki Hatakenaka,[1,3] Susumu Kurihara,[4] and Anton Zeilinger[5]
[1]*Graduate School of Integrated Arts and Sciences, Hiroshima University, Higashi-Hiroshima 739-8521, Japan*
[2]*Research Institute for Science and Engineering, Waseda University, Shinjuku-ku, Tokyo 169-8555, Japan*
[3]*Center for Education and Research for Topological Science and Technology, Hokkaido University, Sapporo 060-8628, Japan*
[4]*Department of Physics, Waseda University, Tokyo 169-8555, Japan*
[5]*Institute of Experimental Physics, University of Vienna, Boltzmanngasse 5, A-1090 Vienna, Austria*
(Received 23 July 2010; revised manuscript received 7 November 2011; published 23 November 2011)

We investigate a quantum-circuit analog of the dynamical Casimir effect discussed in cavity quantum electrodynamics (QED). A double superconducting quantum interference device (SQUID), consisting of a superconducting loop interrupted by a dc-SQUID, is regarded as a harmonic oscillator with a time-dependent frequency imitating the nonadiabatic boundaries in a cavity QED. Squeezing occurs due to parametric processes inherent in the system. We reformulate squeezing based on the Bogoliubov transformation between eigenstates at different times and derive the analytic formula for quantum-state evolutions of the system. The squeezing parameter clearly reveals the relationship between squeezing and nonadiabatic nature of the system. Thus, the squeezing parameter serves as a measure for the dynamical Casimir effect. We demonstrate squeezing for two types of frequency modulation and propose a method for measuring squeezing by using a circuit QED technique under coherent oscillations between an artificial atom and an LC circuit in the presence of dissipation. These observations suggest that a quantum circuit with a Josephson junction is a promising candidate for detecting the dynamical Casimir effect.

DOI: 10.1103/PhysRevB.84.174521 PACS number(s): 85.25.Dq, 42.50.Lc, 42.50.Dv

I. INTRODUCTION

In classical mechanics, a vacuum is an empty space, whereas, in quantum field theory, the vacuum is not truly empty but instead contains virtual particles that are created and annihilated from the vacuum due to fluctuations in the zero-point energy or the vacuum energy. Casimir revealed the zero-point fluctuations by predicting an attractive force between uncharged metallic plates in a vacuum.[1] This was confirmed experimentally by Lamoreaux and Mohideen *et al.*.[2,3]

The dynamical counterpart of the Casimir effect (the dynamical Casimir effect) is also a key problem in terms of exploiting the nature of vacuum fluctuations of electromagnetic fields in the time domain. Moore predicted that real photons could be created from the vacuum fluctuations in an electromagnetic resonator with moving boundaries[4] [see Fig. 1(a)]. However, the effect has not been verified experimentally mainly due to the difficulty in moving the mirror at a fast-enough speed to generate photons.

Yablonovich proposed a new approach for realizing moving boundaries without moving mirrors.[5] The idea is based on the rapid changes of the refractive index in a semiconductor cavity through conductance modulations due to electron-hole pairs generated by optical pulse irradiation. However, the extra charges from the electron-hole pairs also lead to undesirable dissipation, resulting in small refractive index changes. This makes the observation difficult.

The idea was expanded in other systems such as the Bose-Einstein condensation of atoms,[6] plasmons,[7] and superconducting devices.[8,9] In particular, a superconducting quantum circuit is a promising candidate for a system to designed imitate the dynamical Casimir effect based on an analog between the Josephson junction and a quantum resonant cavity, pointed out first by Dodonov *et al.*.[10–14] Both systems can be modeled as harmonic oscillators with time-dependent frequencies [see Fig. 1(b)]. Such time-dependent harmonic oscillators (TDHOs)[15–18] exhibit parametric amplification due to the temporal modification of a system parameter.[19] The parametric amplification differs from usual amplification caused by an actual force acting on the system. In other words, it is impossible to excite a TDHO initially when it is at rest in classical regime. In contrast, the TDHO in quantum-mechanical regimes cannot be at rest because of zero-point fluctuations, which are purely quantum-mechanical effect that are capable of exciting the system. Therefore, the dynamical Casimir effect can be regarded as the parametric amplification of zero-point fluctuations of electromagnetic fields in the cavity.

Using the same idea, we have proposed a concrete system for creating a TDHO using superconducting quantum circuits, including Josephson junctions. We regard our proposed system as an artificial atom with a tunable frequency as well as strong coupling to electromagnetic fields. This allows us to achieve the rapid change in the system frequency required for producing a nonadiabatic boundary effect of the order of several tens of picoseconds with the rapid single flux quantum (RSFQ) technique.[20] In addition, strong coupling facilitates the detection of the effect. Furthermore, the Josephson system operates at sufficiently low temperatures and then suppress the generation of the photons by the parametric amplification of the thermal noise.

In our previous article,[21,22] we demonstrated numerically squeezed-state generation as a result of the quantum-state evolution of the system under nonadiabatic processes only for specific parameters. In this article, we investigate the nonadiabatic processes in the TDHO system for a wide parameter range and analytically formulate the quantum-state evolution of the TDHO system to elucidate the mechanism of squeezed-state generation caused by nonadiabatic processes.

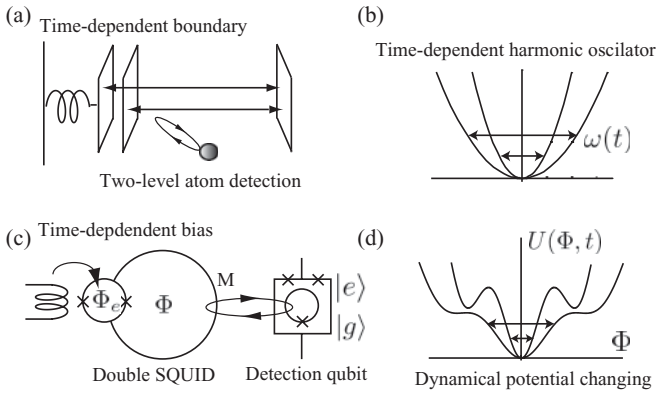

FIG. 1. (a) The moving boundary and two-level atom for detecting the dynamical Casimir effect. (b) The time-dependent harmonic potential. (c) Schematics of a double SQUID. (d) Potential energy of a double SQUID and its dynamical motion. The potential is normalized by the Josephson energy $E_J = \hbar I_0/2e$.

We also provide a more effective and practical way of nonadiabatic biasing for demonstrating the dynamical Casimir effect.

II. JOSEPHSON ARTIFICIAL ATOMS

The system we consider here consists of a superconducting loop with an inductance L interrupted by a dc superconducting quantum interference device (SQUID) with capacitance C (double SQUID)[23,24] shown in Fig. 1(c). $\hat{\Phi}$ and Φ_e represent the magnetic flux threading the large and small loops, respectively.

The double SQUID behaves as an rf-SQUID with a tunable Josephson critical current because the dc-SQUID can be regarded as a single Josephson junction with a variable critical current $I_c(t) = I_0 \cos[2\pi\Phi_e(t)/\Phi_0]$ with I_0 and Φ_0, respectively, being the Josephson critical current and the flux quantum defined as $\Phi_0 = h/2e$. The elementary charge and Planck's constant are denoted as e and h, respectively. Figure 1(d) shows the potential profile as a function of $\hat{\Phi}$ at various $I_c(t)$ values. The motion of the magnetic flux $\hat{\Phi}$ is described by a particle in the potential

$$\hat{U}(\hat{\Phi},t) = \frac{\hbar I_c(t)}{2e}\left(1 - \cos 2\pi\frac{\hat{\Phi}}{\Phi_0}\right) + \frac{\hat{\Phi}^2}{2L}. \tag{1}$$

This potential is expanded up to fourth order on $\hat{\Phi}$,

$$\hat{U}(\hat{\Phi},t) \simeq \frac{1}{2L}\left[1 + \left(2\pi\frac{LI_c(t)}{\Phi_0}\right)\right]\hat{\Phi}^2 - \frac{I_c(t)\pi^3}{3\Phi_0^3}\hat{\Phi}^4. \tag{2}$$

This system is considered to be a harmonic oscillator with a time-dependent frequency when the fourth-order term is negligible. This frequency $\omega(t)$ can be controlled by the external flux bias Φ_e, ranging from 0 to 363 GHz for the typical junction parameters, $C = 0.5$ pF, $I_0 = 20$ μA, and $L = 200$ pH.[25]

Note that there is a lower bound for this frequency, even if it could be $\omega(t) \simeq 0$ in principle, since the fourth-order term in Eq. (2) becomes appreciable compared with the second-order term when the frequency is small. As a result, the harmonic approximation breaks down for such a small frequency. The lower bound is determined as follows. The ratio of the fourth to the second-order terms in Eq. (2) is given as

$$\frac{I_c(t)\pi^3\hat{\Phi}^4/(3\Phi_0^3)}{C\omega(t)^2\hat{\Phi}^2/2} = \frac{2\pi^3}{3}\frac{L_J(t)I_c(t)}{\Phi_0}\left(\frac{\hat{\Phi}}{\Phi_0}\right)^2, \tag{3}$$

where $L_J(t) = 1/[C\omega(t)^2]$ is the effective inductance of the double SQUID. This ratio depends on $\hat{\Phi}$ as expected. Here we evaluate this ratio at classical turning points given as $\Phi_c = [(2n+1)\hbar/C\omega(t)]^{1/2}$:

$$\frac{2\pi^3}{3}\frac{L_J(t)I_c(t)}{\Phi_0}\left(\frac{\hat{\Phi}}{\Phi_0}\right)^2 = \frac{2\pi}{3}\frac{L_J(t)I_c(t)}{\Phi_0}\frac{E_C}{\hbar\omega(t)}\left(n+\frac{1}{2}\right), \tag{4}$$

where $E_C = (2e)^2/2C$ is a charging energy corresponding to a single Cooper pair. The ratio of the fourth order to the second order at $n = 10$ is only a few percentage points when $\omega(t)/2\pi = 10$ GHz. Therefore, the double SQUID can be regarded as a TDHO to at least $n = 10$. The nonlinear effect will be discussed elsewhere.

Now let us define the annihilation and creation operators at time $t = 0$ as

$$\hat{a} = \sqrt{\frac{C\omega_0}{2\hbar}}\hat{\Phi} + i\sqrt{\frac{1}{2\hbar C\omega_0}}\hat{Q}, \tag{5}$$

$$\hat{a}^\dagger = \sqrt{\frac{C\omega_0}{2\hbar}}\hat{\Phi} - i\sqrt{\frac{1}{2\hbar C\omega_0}}\hat{Q}, \tag{6}$$

where $\omega_0 = \omega(t=0)$ is an initial frequency and $\hat{Q}$ is an electric charge on the junction capacitor. By using $\hat{a}$ and $\hat{a}^\dagger$, the Hamiltonian at time t is written as

$$\hat{H}(t) = \frac{\hbar\omega_0}{4}\left(\left[\left(\frac{\omega(t)}{\omega_0}\right)^2 + 1\right](\hat{a}^\dagger\hat{a} + \hat{a}\hat{a}^\dagger) + \left\{\left[\frac{\omega(t)}{\omega_0}\right]^2 - 1\right\}(\hat{a}^{\dagger 2} + \hat{a}^2)\right). \tag{7}$$

This is diagonalized as

$$\hat{H}(t) = \frac{\hbar\omega(t)}{2}[\hat{b}^\dagger(t)\hat{b}(t) + \hat{b}(t)\hat{b}^\dagger(t)] \tag{8}$$

by using the Bogoliubov transformation,

$$\hat{b}(t) = \hat{V}(t)\hat{a}\hat{V}^\dagger(t), \tag{9}$$

$$\hat{b}(t)^\dagger = \hat{V}(t)\hat{a}^\dagger\hat{V}^\dagger(t), \tag{10}$$

with

$$\hat{V}(t) = \exp\left[-\frac{\mu(t)}{2}(\hat{a}^2 - \hat{a}^{\dagger 2})\right], \tag{11}$$

$$\mu(t) = -\frac{1}{2}\ln\left(\frac{\omega(t)}{\omega_0}\right). \tag{12}$$

The number state $|n(t)\rangle$ at time t defined by the snapshot number operator $\hat{b}^\dagger(t)\hat{b}(t)$ is generated by the operator $\hat{V}(t)$ from number state $|n\rangle$ at time $t = 0$, i.e., $|n(t)\rangle = \hat{V}(t)|n\rangle$. In other words, the unitary operator $\hat{V}(t)$ is regarded as a time-translational operator for the basis and it represents the fact that the definition of the eigenstate changes over time.

III. QUANTUM-STATE EVOLUTIONS

Let us consider the time evolution of the state $|\phi(t)\rangle$, which is initially prepared in the ground state $|0\rangle$. The state $|\phi(t)\rangle$ at time t is expressed in terms of the snapshot eigenstates $|n(t)\rangle$, i.e., $|\phi(t)\rangle = \sum_{n=0} C_n(t)|n(t)\rangle$, with $C_n(t)$ being the time-dependent expansion coefficient for n-th snapshot number state. In this expansion, both the coefficient and basis are time dependent. To focus on the time evolution of $C_n(t)$ by excluding the time evolution of the basis, we apply the operator $\hat{V}^\dagger(t)$ to $|\phi(t)\rangle$ and define the state $|\tilde{\phi}(t)\rangle \equiv \hat{V}^\dagger(t)|\phi(t)\rangle$, which is governed by the Schrödinger equation

$$\begin{aligned} i\hbar\frac{\partial}{\partial t}|\tilde{\phi}(t)\rangle &= \left[\hat{V}^\dagger(t)\hat{H}(t)\hat{V}(t) - i\hbar\hat{V}^\dagger(t)\frac{\partial}{\partial t}\hat{V}(t)\right]|\tilde{\phi}(t)\rangle \\ &= \left[\hbar\omega(t)\left(\hat{a}^\dagger\hat{a}+\frac{1}{2}\right)+i\frac{\hbar\dot{\mu}(t)}{2}(\hat{a}^2-\hat{a}^{\dagger 2})\right]|\tilde{\phi}(t)\rangle \\ &\equiv \{\hat{H}_0(t)+\hat{H}_{\rm na}(t)\}|\tilde{\phi}(t)\rangle \end{aligned} \tag{13}$$

with

$$\dot{\mu}(t) = -\frac{1}{2}\frac{d}{dt}\left\{\ln\left[\frac{\omega(t)}{\omega_0}\right]\right\} = -\frac{1}{2}\frac{\dot{\omega}(t)}{\omega(t)}. \tag{14}$$

The second term $\hat{H}_{\rm na}(t)$ on the right-hand side of Eq. (13) is proportional to $\dot{\omega}(t)/\omega(t)$, which shows the nonadiabatic effect that excites the system to even-numbered levels. Thus, the state $|\tilde{\phi}(t)\rangle$ no longer stays in the ground state when $\hat{H}_{\rm na}(t)$ becomes significant. The Hamiltonian $\hat{H}_{\rm na}(t)$ is equivalent to the squeezed Hamiltonian in nonlinear quantum optics.[26] Therefore, the squeezed-state generation due to nonadiabatic boundary changes is clear evidence demonstrating the dynamical Casimir effect in Josephson artificial atoms.

IV. NONADIABATIC EFFECT AND SQUEEZING

To investigate the effect of $H_{\rm na}(t)$, we move to the interaction picture, $|\tilde{\phi}(t)\rangle = U_0(t)|\tilde{\phi}(t)\rangle_{\rm int}$ with $U_0(t) = \exp[-\frac{i}{\hbar}\int_0^t \hat{H}_0(t')dt']$. The time evolution of $|\tilde{\phi}(t)\rangle_{\rm int}$ due to the nonadiabatic effect is governed by the equation

$$i\hbar\frac{\partial}{\partial t}|\tilde{\phi}(t)\rangle_{\rm int} = \hat{H}^{\rm int}_{\rm na}(t)|\tilde{\phi}(t)\rangle_{\rm int}, \tag{15}$$

with

$$\begin{aligned} \hat{H}^{\rm int}_{\rm na}(t) &= \hat{U}_0^\dagger(t)\hat{H}_{\rm na}(t)\hat{U}_0(t) \\ &= i\frac{\hbar\dot{\mu}(t)}{2}[\hat{a}^2 e^{-2i\int_0^t\omega(t')dt'} - \text{H.c.}]. \end{aligned} \tag{16}$$

Here H.c. is the Hermitian conjugate of the terms in parentheses. The formal solution of this equation is expressed by

$$\begin{aligned} |\tilde{\phi}(t)\rangle_{\rm int} &= \hat{T}\exp\left[-\frac{i}{\hbar}\int_0^t \hat{H}^{\rm int}_{\rm na}(t')dt'\right]|0\rangle \\ &\equiv \hat{U}(t)|0\rangle, \end{aligned} \tag{17}$$

where $\hat{T}$ is a time-ordering operator and $U(t)$ is an exact time evolution operator. However, it is difficult to obtain an analytical solution for Eq. (15) because the Hamiltonian cannot commute itself at different times. Hereafter, we consider the situation where

$$\begin{aligned} &\left[\hat{H}^{\rm int}_{\rm na}(t), \hat{H}^{\rm int}_{\rm na}(t')\right] \\ &= i\hbar^2\dot{\mu}(t)\dot{\mu}(t')\sin\left[\int_{t'}^t \omega(t'')dt''\right](\hat{a}^\dagger\hat{a}+\hat{a}\hat{a}^\dagger). \\ &\simeq 0. \end{aligned} \tag{18}$$

This appears to be appropriate with both adiabatic and nonadiabatic limits. For an adiabatic situation, Eq. (18) is satisfied due to the small $\dot{\mu}(t)$ from the definition. While in a nonadiabatic case, $\dot{\mu}(t)$ is localized in the time domain due to quick frequency changes. The product $\dot{\mu}(t)\dot{\mu}(t')$ in Eq. (18) becomes small when t and t' are temporally distant. On the other hand, $\sin[\int_{t'}^t \omega(t'')dt'']$ becomes small when $t \simeq t'$. Thus, these make the commutation relation on Hamiltonian in different times commutative.

Under the above conditions, we obtain an approximate solution by omitting the time-ordering operator from Eq. (17),

$$\begin{aligned} |\phi(t)\rangle_{\rm int} &\simeq \exp\left[-\frac{i}{\hbar}\int_0^t \hat{H}^{\rm int}_{\rm na}(t')dt'\right]|0\rangle \\ &= \exp\left[\frac{1}{2}\int_0^t \dot{\mu}(t)[\hat{a}^2 e^{-2i\int_0^t\omega(t')dt'} - \text{H.c.}]dt'\right]|0\rangle \\ &\equiv \hat{U}_{\rm app}(t)|0\rangle, \end{aligned} \tag{19}$$

where $\hat{U}_{\rm app}(t)$ is an approximate time evolution operator. In this approximation, a state with time-dependent bases at time t is obtained by multiplying the operator $\hat{V}(\mu)$ by the approximate solution $|\tilde{\phi}(t)\rangle = \hat{U}_0(t)|\tilde{\phi}(t)\rangle_{\rm int}$,

$$\begin{aligned} |\phi(t)\rangle &= \hat{V}(t)\hat{U}_0(t)|\tilde{\phi}(t)\rangle_{\rm int} \\ &= \hat{V}(t)\hat{U}_0(t)\exp\left[-\frac{i}{\hbar}\int_0^t \hat{H}^{\rm int}_{\rm na}(t')dt'\right]\hat{U}_0^\dagger(t)\hat{U}_0|0\rangle \\ &= \hat{V}(t)\exp\left[-\frac{i}{\hbar}\int_0^t \hat{U}_0(t)\hat{H}^{\rm int}_{\rm na}(t')\hat{U}_0^\dagger(t)dt'\right] \\ &\quad\times e^{-\frac{i}{2}\int_{t'}^t\omega(t')dt'}|0\rangle \\ &= e^{-\frac{i}{2}\int_{t'}^t\omega(t')dt'}\hat{V}(t) \\ &\quad\times\exp\left[\frac{1}{2}\int_0^t \dot{\mu}(t')[\hat{a}^2 e^{-2i\int_t^{t'}\omega(t'')dt''} - \text{H.c.}]dt'\right] \\ &\quad\times\hat{V}^\dagger(t)\hat{V}(t)|0\rangle \\ &= e^{-\frac{i}{2}\int_0^t\omega(t')dt'}e^{-\frac{1}{2}\{\nu\hat{b}(t)^2-\nu^*\hat{b}^\dagger(t)^2\}}|0(t)\rangle. \end{aligned} \tag{20}$$

Here we use Eqs. (9) and (10) and $\hat{V}(t)|0\rangle = |0(t)\rangle$. This is simply *the squeezed vacuum state* with the squeezing parameter

$$\begin{aligned} \nu(t) &= \int_0^t \dot{\mu}(t'-t_0)e^{2i\int_t^{t'}\omega(t'')dt''}dt' \\ &= \frac{1}{2}\int_0^t \frac{\dot{\omega}(t')}{\omega(t')}e^{2i\int_t^{t'}\omega(t'')dt''}dt'. \end{aligned} \tag{21}$$

This is our main result. The nonadiabatic effect $\dot{\omega}(t')/\omega(t')$ is connected to squeezing parameter $\nu(t)$. Therefore, the dynamical counterpart of the Casimir effect can be confirmed by investigating the squeezing of the quantum flux in the double SQUID. Interestingly, this is identical to Dodonov's

expression[27] for the amplitude reflection coefficient for the effective barrier of the time-dependent pulse potential.

Here we consider our approximation in more detail. The difference between the approximate time-evolution operator Eq. (19) and the exact time-evolution operator Eq. (17) is expressed up to the second order of the Hamiltonian,

$$\hat{U}_{\rm app}(t)-\hat{U}(t) = \frac{1}{2}\left(\frac{1}{i\hbar}\right)^2\int_0^t dt'\int_{t'}^t dt''\left[\hat{H}_{\rm na}^{\rm int}(t'),\hat{H}_{\rm na}^{\rm int}(t'')\right]. \quad (22)$$

By operating $\hat{U}_{\rm app}^{\dagger}(t)$ on both sides of Eq. (22), this reduces to

$$\begin{aligned}\hat{U}(t)\hat{U}_{\rm app}^{\dagger}(t) &= 1-\frac{1}{2}\left(\frac{1}{i\hbar}\right)^2\int_0^t dt'\int_{t'}^t dt''\left[\hat{H}_{\rm na}^{\rm int}(t'),\hat{H}_{\rm na}^{\rm int}(t'')\right]U_{\rm app}^{\dagger}(t)\\ &\quad+O\left[\left(\hat{H}_{\rm na}^{\rm int}\right)^3\right]\\ &= \exp\left\{-\frac{1}{2}\left(\frac{1}{i\hbar}\right)^2\int_0^t dt'\int_{t'}^t dt''\left[\hat{H}_{\rm na}^{\rm int}(t'),\hat{H}_{\rm na}^{\rm int}(t'')\right]\right\}\\ &\quad+O\left[\left(\hat{H}_{\rm na}^{\rm int}\right)^3\right]. \quad (23)\end{aligned}$$

Equivalently,

$$\begin{aligned}\hat{U}(t) &= \exp\left\{-\frac{1}{2}\left(\frac{1}{i\hbar}\right)^2\int_0^t dt'\int_{t'}^t dt''\left[\hat{H}_{\rm na}^{\rm int}(t'),\hat{H}_{\rm na}^{\rm int}(t'')\right]\right\}\\ &\quad\times\hat{U}_{\rm app}(t)+O\left[\left(\hat{H}_{\rm na}^{\rm int}\right)^3\right]\\ &= \exp\left\{\frac{i}{2}\int_0^t dt'\int_{t'}^t dt''\dot{\mu}(t)\dot{\mu}(t')\sin\left(\int_{t'}^t\omega(t'')dt''\right)\right.\\ &\quad\left.\times(\hat{a}^{\dagger}\hat{a}+\hat{a}\hat{a}^{\dagger})\right\}\hat{U}_{\rm app}(t)+O\left[\left(\hat{H}_{\rm na}^{\rm int}\right)^3\right], \quad (24)\end{aligned}$$

where we use the commutation relation $[\hat{H}_{\rm na}^{\rm int}(t'),\hat{H}_{\rm na}^{\rm int}(t'')]$ given as Eq. (18). The correction changes only the phase of the squeezing parameter. Therefore, the approximate solution for the squeezing parameter is correct up to the second order of the Hamiltonian as regards its absolute value.

Let us consider two different types of frequency modulations as concrete examples: (i) the frequency $\omega(t)$ monotonically decreases from ω_0 to ω_1 (single-step frequency modulation) and (ii) the frequency $\omega(t)$ sinusoidally oscillates in time (sinusoidal frequency modulation).

1. Single-step frequency modulation

As a first simple example, we investigate the quantum-state evolutions of a flux particle in a double SQUID for a single-step frequency modulation given as

$$\begin{aligned}\omega(t-t_0) &= \frac{\omega_0+\omega_1}{2}-\frac{\omega_0-\omega_1}{2}\tanh\left\{\frac{2(t-t_0)}{\tau}\right\}\\ &\equiv \omega_+-\omega_-\tanh\left\{\frac{2(t-t_0)}{\tau}\right\}, \quad (25)\end{aligned}$$

where $\omega_{\pm}=(\omega_0\pm\omega_1)/2$. The hyperbolic tangent is introduced solely to avoid any numerical divergence in the calculations. The frequency $\omega(t)$ monotonically changes from ω_0 to ω_1 in the duration τ as shown in Fig. 2(a). The

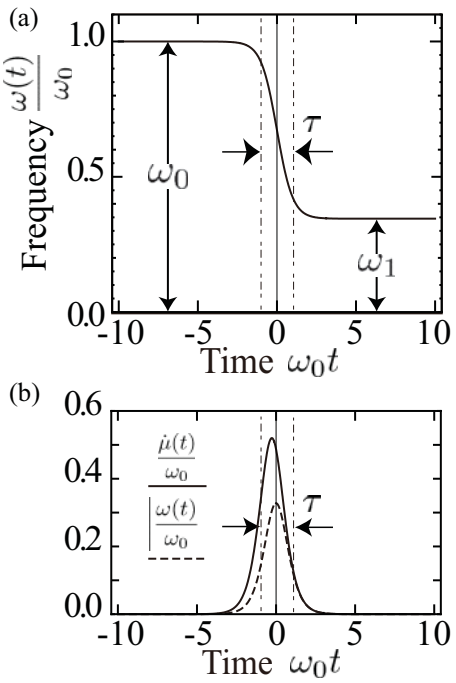

FIG. 2. (a) Temporal profile of $\omega(t)$. (b) Temporal profile of $\dot{\mu}(t)=-(1/2)[\dot{\omega}(t)/\omega(t)]$ (solid line) and $-\dot{\omega}(t)$ (dashed line).

corresponding $\dot{\mu}(t)$ together with $\dot{\omega}(t)$ are also depicted in Fig. 2(b). We performed numerical calculations using a procedure described in our previous article.[21,22] The numerically obtained distribution probabilities $P_n(t)=|C_n(t)|^2$ are well fitted by a super-Poissonian distribution in a squeezed vacuum state[26]

$$P_n(t)=\frac{\sinh^n(|\nu(t)|)}{2^n n!\cosh^{n+1}(|\nu(t)|)}H_n(0)^2, \quad (26)$$

where $H_n(x)$ is the nth-degree Hermite polynomial.

Figure 3 shows the absolute values of squeezing parameter $|\nu(t)|$ at $t=\infty$ as a function of a normalized modulation rate $1/\omega_0\tau$ for a sudden frequency change. Our approximate solutions agree well with numerical results obtained by the fitting of the distribution of the number states.[22] In the nonadiabatic limit ($\tau\ll 1/\omega_0, 1/\omega_1$), the squeezing parameter approaches an asymptotic value as shown in Fig. 3. This can be estimated as follows. In the single-step frequency modulation, $\dot{\mu}(t'-t_0)$ in Eq. (21) is localized as shown in Fig. 2(b). Thus, the exponent in Eq. (21) can be expanded around $t'=t_0$ up to the first order of $(t'-t_0)$,

$$\begin{aligned}&2i\int_t^{t'}\omega(t''-t_0)dt''\\ &\simeq 2i\int_t^{t_0}\omega(t''-t_0)dt''+2i(t'-t_0)\omega_+\\ &=-2i(t-t_0)\omega_++\frac{\tau\omega_-}{2}\ln\left[\cosh(t-t_0)/\tau\right]+2i(t'-t_0)\omega_+. \quad (27)\end{aligned}$$

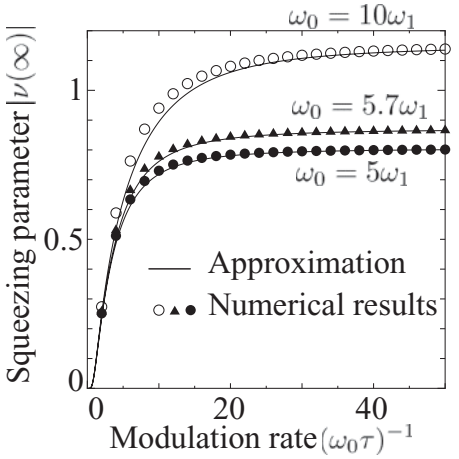

FIG. 3. The squeezing parameter as a function of the modulation rates for single-step modulation. The dots are numerical solutions and the solid lines are approximate solutions, Eq. (21).

Under this approximation, the squeezing parameter becomes

$$\begin{aligned}
\nu(t) &= \int_0^t \dot{\mu}(t'-t_0)e^{2i\int_t^{t'}\omega(t''-t_0)dt''}dt' \\
&\simeq e^{2i\int_t^{t_0}\omega(t''-t_0)dt''}\int_0^t \dot{\mu}(t'-t_0)e^{2i(t'-t_0)\omega_+}dt' \\
&\simeq e^{2i\int_t^{t_0}\omega(t''-t_0)dt''} \\
&\quad\times\int_0^t \dot{\mu}(t'-t_0)[1+2i(t'-t_0)\omega_+ +\cdots]dt' + O(\tau\omega_+) \\
&\simeq e^{2i\int_t^{t_0}\omega(t''-t_0)dt''} \\
&\quad\times\left[\int_0^t \dot{\mu}(t'-t_0)dt' + i\omega_+\dot{\mu}(0)\int_{t_0}^{t_0+\tau/2}(t'-t_0)dt'\right] \\
&\quad + O(\tau\omega_+) \\
&\simeq e^{2i\int_t^{t_0}\omega(t''-t_0)dt''}\left[\mu(t) + i\omega_+\frac{1}{\tau}\frac{\omega_-}{\omega_+}\frac{\tau^2}{2}\right] + O(\tau\omega_+) \\
&= e^{2i\int_t^{t_0}\omega(t''-t_0)dt''}\mu(t) + O(\tau\omega_+). \qquad (28)
\end{aligned}$$

With the limit of a small $\tau\omega_+$, namely the nonadiabatic limit, the absolute value of the squeezing parameter observed in the Fig. 3 is given as

$$|\nu(t=\infty)| = |\mu(t=\infty)| = \frac{1}{2}\ln\left(\frac{\omega_0}{\omega_1}\right), \qquad (29)$$

where $\omega_1 = \omega(t=\infty)$.

With the opposite limit($\tau \gg 1/\omega_0, 1/\omega_1$), the approximate solution also works well since a small $\dot{\mu}(t)$ makes the approximation $[\hat{H}_{\rm na}^{\rm int}(t), \hat{H}_{\rm na}^{\rm int}(t')] \simeq 0$ reasonable. In this situation, $\omega(t) \simeq \omega_+ - 2t\omega_-/\tau$ in Eq. (21). The squeezing parameter becomes

$$\begin{aligned}
\nu(t) &= \int_0^t \dot{\mu}(t'-t_0)e^{2i\int_t^{t'}\omega(t''-t_0)dt''}dt' \\
&\simeq \frac{-1}{2}\int_{-t_0}^{t-t_0}\frac{\dot{\omega}(t')}{\omega(t')}e^{2i\int_{t-t_0}^{t'}\omega(t'')dt''}dt' \\
&\simeq \frac{1}{2}\int_{-t_0}^{t-t_0}\frac{2\omega_-\left(\frac{1}{\tau}\right)}{\omega_+ - 2t'\omega_-\left(\frac{1}{\tau}\right)}e^{2i[t'\omega_+ - t'^2\omega_-(\frac{1}{\tau})]}dt' \\
&= \frac{1}{2}\int_{-t_0}^{t-t_0}\frac{2\left(\frac{\omega_-}{\omega_+}\right)\left(\frac{1}{\tau}\right)}{1-2t'\left(\frac{\omega_-}{\omega_+}\right)\left(\frac{1}{\tau}\right)}e^{-i\omega_-\frac{1}{\tau}\left[t'-\left(\frac{\omega_+}{\omega_-}\tau\right)\right]^2 + \frac{i\tau\omega_-}{2}\left(\frac{\omega_+}{\omega_-}\right)^2}dt' \\
&\simeq \left(\frac{\omega_-}{\omega_+}\right)\frac{1}{\tau}\int_{-t_0}^{t-t_0}e^{-2i\frac{\omega_-}{\tau}\left[t'-\frac{\tau}{2}\left(\frac{\omega_+}{\omega_-}\right)\right]^2 + \frac{i\tau\omega_-}{2}\left(\frac{\omega_+}{\omega_-}\right)^2}dt' \\
&\simeq \left(\frac{\omega_-}{\omega_+}\right)\sqrt{\frac{\pi}{2i\tau\omega_-}}e^{i\frac{\tau\omega_-}{2}\left(\frac{\omega_+}{\omega_-}\right)^2} \\
&\propto \frac{1}{\sqrt{\tau}}, \qquad (30)
\end{aligned}$$

where we took the limit $t_0 \to \infty$. Therefore, squeezing does not occur in the adiabatic limit $\tau \to \infty$.

Let us now estimate the absolute value of the maximum squeezing parameter using realistic junction parameters. By using Eq. (29), it becomes 0.89 when we employ $\omega_0/2\pi = 57$ GHz and $\omega_1/2\pi = 10$ GHz with a subpicosecond changing duration τ, say 0.8 ps,[28] which was achieved in recent experiments using femtosecond photoexcitation techniques. In this case, the product $\tau\omega_+$ yields 0.17, which is sufficiently small for us to ignore $O(\tau\omega_+)$ in Eq. (28). This squeezing parameter corresponds to the average excited photon number, which is calculated from the population distribution of Eq. (26), $\langle\hat{a}^\dagger\hat{a}\rangle = \sinh^2|\nu| = 0.97$. Therefore, the nonadiabatic effect is sufficiently strong to generate one photon in the above situation.

2. *Sinusoidal frequency modulation*

The single-step frequency modulation scheme most clearly uncovers the nonadiabatic effect of the system, but it is practically ineffective because the entire nonadiabatic effect is generated solely by a one-time frequency modulation. In addition, it requires ultrafast system controls. Here we consider an alternative scheme, i.e., a sinusoidal frequency modulation given as

$$\omega(t) = \omega_0 + \delta\omega\sin\omega t, \qquad (31)$$

where $\delta\omega$ is the modulation amplitude. This frequency modulation is conventional and the nonadiabatic effect is expected to be accumulated in periodic cycles.

Figure 4 shows the time evolution of $\nu(t)$ with $\delta\omega/\omega_0 = 0.04$, for example. The squeezing parameter oscillation increases with in time in this sinusoidal frequency modulation. The increase rate is calculated as follows. By substituting the sinusoidal $\omega(t)$ into Eq. (21), the squeezing parameter is calculated as

$$\begin{aligned}
\nu(t) &= \frac{1}{2}\int_0^t \frac{\dot{\omega}(t')}{\omega(t')}e^{2i\int_t^{t'}\omega(t'')dt''}dt' \\
&= \frac{1}{2}\sum_{s,p=-\infty}^{\infty} c_s J_p\left(2\frac{\delta\omega}{\omega}\right)(-i)^p e^{2i\frac{\delta\omega}{\omega}}\int_0^t e^{it[(s+p)\omega+2\omega_0]}dt' \\
&= \frac{1}{2}\sum_{s,p=-\infty}^{\infty} c_s J_p\left(2\frac{\delta\omega}{\omega}\right)(-i)^p e^{2i\frac{\delta\omega}{\omega}} \\
&\quad\times\frac{\sin\{t[(s+p)\omega+2\omega_0]/2\}}{[(s+p)\omega+2\omega_0]/2}e^{it[(s+p)\omega+2\omega_0]/2}
\end{aligned}$$

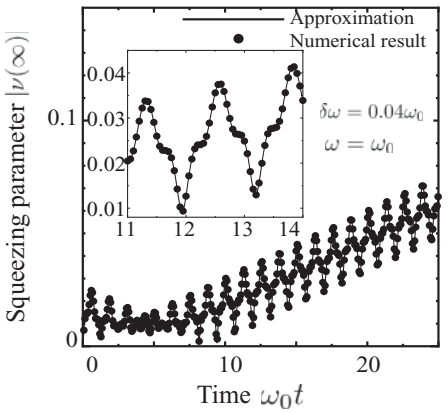

FIG. 4. Time evolution of the squeezing parameter for sinusoidal change $[\omega(t) = \omega_0 + \delta\omega \sin\omega t]$. The dots are numerical solutions and the solid lines correspond to the approximate solution.

$$= \frac{1}{2}\sum_{l,p=-\infty}^{\infty} c_{l-p} J_p\left(2\frac{\delta\omega}{\omega}\right)(-i)^p e^{2i\frac{\delta\omega}{\omega}} \times \frac{\sin\left[t(l\omega+2\omega_0)/2\right]}{(l\omega+2\omega_0)/2} e^{it(l\omega+2\omega_0)/2}. \quad (32)$$

Here we use the Fourier expansion for $\dot{\omega}(t)/\omega(t)$ as

$$\frac{\dot{\omega}(t)}{\omega(t)} = \frac{\delta\omega\omega\cos\omega t}{\omega_0 + \delta\omega\sin\omega t} = \sum_{s=-\infty}^{\infty} c_s e^{is\omega t}, \quad (33)$$

where the Fourier components are given as

$$c_s = \begin{cases} i\omega(-ia)^s & \text{for } s > 0 \\ 0 & \text{for } s = 0 \\ -i\omega(ia)^{-s} & \text{for } s < 0 \end{cases} \quad (34)$$

and are roughly proportional to the modulation amplitude $\delta\omega$ from the definition of the parameter a,

$$a = \frac{\left(\frac{\delta\omega}{\omega_0}\right)}{1+\sqrt{1-\left(\frac{\delta\omega}{\omega_0}\right)^2}} < 1. \quad (35)$$

The rotating phase term, $\exp\left[2i\int_0^t \omega(t')dt'\right]$, is also expanded as

$$\exp\left[2i\int_0^t \omega(t')dt'\right] = \sum_{p=-\infty}^{\infty} J_p\left(2\frac{\delta\omega}{\omega}\right)(-i)^p e^{ip\omega t} e^{-2i\left(\omega_0 t - \frac{\delta\omega}{\omega}\right)}, \quad (36)$$

where $J_p(x)$ is the pth-order Bessel function.

The last sine term in Eq. (32) represents an energy conservation rule $l\omega + 2\omega_0 = 0$ and increases linearly with time when the modulation frequency ω satisfies $n\omega = 2\omega_0$ with n being an integer, i.e., $l\omega + 2\omega_0 = \omega(l+n) = 0$ for $l = -n$. Otherwise, the sine term oscillates at any l except $l = -n$, resulting in no squeezing. The squeezing parameter can be divided into a t-linear term $\nu_{\rm lin}(t)$ for $l = -n$ and an oscillating term $\delta\nu(t)$ for any l except $l = -n$,

$$\begin{aligned}\nu(t) &= \frac{1}{2}\sum_{l,p=-\infty}^{\infty} c_{l-p} J_p\left(2\frac{\delta\omega}{\omega}\right)(-i)^p e^{2i\frac{\delta\omega}{\omega}} \times \frac{\sin\left[t(l\omega+2\omega_0)/2\right]}{(l\omega+2\omega_0)/2} e^{it(l\omega+2\omega_0)/2} \\ &= \frac{1}{2}\sum_{p=-\infty}^{\infty} c_{-n-p} J_p\left(2\frac{\delta\omega}{\omega}\right)(-i)^p e^{2i\frac{\delta\omega}{\omega}} \times t \\ &\quad + \frac{1}{2}\sum_{p=-\infty, l\neq -n}^{\infty} c_{l-p} J_p\left(2\frac{\delta\omega}{\omega}\right)(-i)^p e^{2i\frac{\delta\omega}{\omega}} \times \frac{\sin\left[t(l\omega+2\omega_0)/2\right]}{(l\omega+2\omega_0)/2} e^{it(l\omega+2\omega_0)/2} \\ &= \nu_{\rm lin}(t) + \delta\nu(t), \end{aligned} \quad (37)$$

where the t-linear term is written as

$$\nu_{\rm lin}(t) = \frac{t}{2} e^{2i\frac{\delta\omega}{\omega}} \sum_{p=-\infty}^{\infty}\left[c_{-n-p} J_p\left(2\frac{\delta\omega}{\omega}\right)(-i)^p\right]. \quad (38)$$

By substituting Eqs. (34) and (36) into Eq. (38), the squeezing rate is analytically obtained as

$$\begin{aligned}\frac{\nu_{\rm lin}(t)}{t} &= \frac{1}{2} e^{2i\frac{\delta\omega}{\omega}} \sum_{p=-\infty}^{\infty} c_{-n-p} J_p\left(2\frac{\delta\omega}{\omega}\right)(-i)^p \\ &= \frac{1}{2} e^{2i\frac{\delta\omega}{\omega}}\left[\sum_{p=-n+1}^{\infty}(-i\omega)(ia)^{p+n}(-i)^p J_p\left(2\frac{\delta\omega}{\omega}\right) + \sum_{p=-\infty}^{-n-1}(i\omega)(-ia)^{-p-n}(-i)^p J_p\left(2\frac{\delta\omega}{\omega}\right)\right] \\ &= \frac{1}{2i} e^{2i\frac{\delta\omega}{\omega}}\omega(-i)^n \times \sum_{r=1}^{\infty}(-a)^r\left[J_{n-r}\left(2\frac{\delta\omega}{\omega}\right) - J_{n+r}\left(2\frac{\delta\omega}{\omega}\right)\right] \\ &\simeq \frac{1}{2i} e^{2i\frac{\delta\omega}{\omega}}\omega(-i)^n \times a\left[J_{n-1}\left(2\frac{\delta\omega}{\omega}\right) - J_{n+1}\left(2\frac{\delta\omega}{\omega}\right)\right] + O(a^2) \\ &= \frac{1}{2i} e^{2i\frac{\delta\omega}{\omega}}\omega(-i)^n a J_n'\left(2\frac{\delta\omega}{\omega}\right) + O(a^2), \end{aligned} \quad (39)$$

where $J_s'(x)$ denotes $[dJ_s(x)/dx]$. Equation (39) has the largest value at $n = 1$ corresponding to $\omega = 2\omega_0$ for other conditions $(n > 1)$ since the differential of the Bessel function $J_s'(2\delta\omega/\omega_0)$ has smaller values as higher orders for a small modulation amplitude $(\delta\omega/\omega_0) \ll 1$, i.e., $J_0'(2\delta\omega/\omega_0) > J_1'(2\delta\omega/\omega_0) > J_2'(2\delta\omega/\omega_0) > \cdots$. Thus, the largest squeezing occurs at $\omega = 2\omega_0$ as shown in Fig. 5.

Note that the resonance we discussed here differs from that of a Rabi oscillation under external alternating fields. An elementary process in Rabi oscillations is essentially a one-photon process together with atomic excitation and relaxation due to the linear coupling between the external field and the

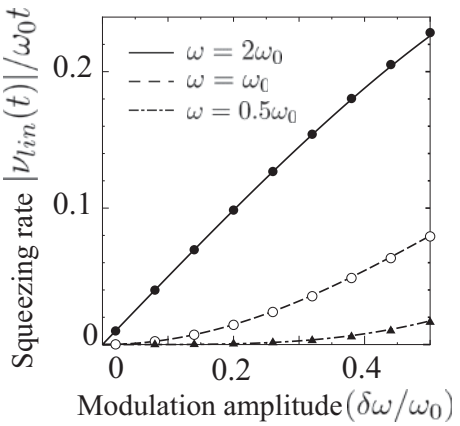

FIG. 5. Squeezing rate $|\nu_{\rm lin}(t)|/\omega_0 t$ as a function of modulation amplitude $\delta\omega/\omega_0$. The black circles, white circles, and black triangles denote numerical results. The solid, dashed, and dotted-dashed lines shows approximate solutions for the time evolution operator.

system described as the Jaynes-Cummings model. Thus, all of the system states of the system are possibly excited. On the other hand, nonadiabatic excitations caused by frequency modulation are regarded as parametric amplifications. This is due to two-photon generation and absorption as shown in Eq. (13). Therefore, the resultant states, i.e., squeezed vacuum states, are excited only in even numbered states.

Let us estimate the elapsed time needed for generating at least the single photon required for observations. The increase rate of the squeezing parameter $|\nu_{\rm lin}(t)|/t$ at $\omega = 2\omega_0$ is roughly $|\nu_{\rm lin}(t)|/t = 0.020\omega_0$ from numerical evaluations of Eq. (32) at $\delta\omega = 0.8$ GHz and $\omega = 40$ GHz. So it is $|\nu_{\rm lin}(t)|/t = 0.40$ GHz at $\omega_0 = 20$ GHz. The photon number in a squeezed state is evaluated as $\langle\hat{a}^\dagger\hat{a}\rangle = \sinh^2|\nu|$. The squeezing parameter corresponding to the $\langle\hat{a}^\dagger\hat{a}\rangle = 1$ is then $|\nu| = \sinh^{-1}1 = 0.88$. The elapsed time required for $|\nu_{\rm lin}(t)| = 0.88$ is a few nanoseconds, for example, 2.2 ns. Recent experiments on quantum circuits with similar circuit parameters support a decoherence time ranging from a few nanoseconds to microseconds. Thus, squeezing grows quickly enough to allow us to detect a photon. As a result, detectable photon generation is also possible in this sinusoidal frequency modulation scheme.

V. MEASUREMENT SCHEME

Let us discuss a detection scheme for squeezed vacuum states generated in a double SQUID. Here we employ the method used in circuit QED experiments[29,30] where, for example, Fock and coherent states in quantum circuits are detected via coupling with a two-state system known as a qubit in quantum information technology.[31] The detection system forms the Jaynes-Cummings model well known in quantum optics. Squeezed vacuum states obtained via the nonadiabatic effect may be detected in a similar experimental scheme to that shown in Fig. 1 (c). The basic idea of this scheme is the quantum-state transfer of a double SQUID into a qubit based on the state-dependent coupling between them peculiar to the Jaynes-Cummings model. Thus, the double SQUID states superimposed in the qubit are analyzed by Fourier transformation.

Below, we analyze the detection scheme in more detail. The quantum state of the double SQUID after nonadiabatic time evolution with an elapsed time t is expressed as $\sum_n C_n(t)|n(t)\rangle$ by using the snapshot number state $|n(t)\rangle$ and the expansion coefficient for the nth snapshot number state. The population distribution $P_n(t) = |C_n(t)|^2$ should be the super-Poissonian distribution in squeezed vacuum states, which is given as Eq. (26).

The qubit is initially prepared at the lower level $|g\rangle$, and then the qubit and double SQUID are tuned into resonance for an adjustable interaction duration τ'. The coupling between the qubit and double SQUID is described by the Jaynes-Cummings Hamiltonian as follows:

$$\hat{H}_{\rm JC} = \hbar\Omega[\hat{b}(t)\hat{\sigma}_+ + \hat{\sigma}_-\hat{b}^\dagger(t)]. \tag{40}$$

Here $\hat{\sigma}_+$ and $\hat{\sigma}_-$ are the qubit raising and lowering operators, respectively. The Rabi frequency is denoted as Ω. The quantum-state evolution of the double SQUID and the qubit in Schrödinger picture is described by the total Hamiltonian

$$\hat{H}_{\rm total} = \hat{H}_s(t) + \hat{H}_{\rm qubit} + \hat{H}_{\rm JC}, \tag{41}$$

where $\hat{H}_s(t)$ is the double SQUID Hamiltonian in Eq. (8). The qubit Hamiltonian is $\hat{H}_{\rm qubit} = \hbar\omega\hat{\sigma}_z/2$, where the Pauli matrix $\hat{\sigma}_z$ is represented in qubit eigenstates basis $|e\rangle$ and $|g\rangle$. The state of the double SQUID and the qubit under the Hamiltonian (41) after time τ' is shown as

$$\begin{aligned}|\phi(\tau')\rangle &= \exp\left(-i\frac{\hat{H}_{\rm total}}{\hbar}\tau'\right)|g\rangle\otimes\sum_n C_n(t)|n(t)\rangle \\ &= \sum_n C_n(t)\Big[e^{-i\left(n-\frac{1}{2}\right)\omega(t)\tau'}\cos\sqrt{n}\Omega\tau'|g\rangle\otimes|n(t)\rangle \\ &\quad - ie^{i\left(n-\frac{1}{2}\right)\omega(t)\tau'}\sin\sqrt{n}\Omega\tau'|e\rangle\otimes|(n-1)(t)\rangle\Big].\end{aligned} \tag{42}$$

The probability $P_e(\tau')$ of finding the qubit in the excited state $|e\rangle$ is given as

$$\begin{aligned}P_e(\tau') &= \sum_n |\{\langle e|\otimes\langle n(t)|\}|\phi(\tau')\rangle|^2 \\ &= \sum_n |C_n(t)|^2\sin^2\Omega\sqrt{n}\tau' \\ &= \sum_n P_n(t)\frac{1-\cos(2\sqrt{n}\Omega\tau')}{2}.\end{aligned} \tag{43}$$

This includes different Fourier components with amplitude $P_n(t)$ and frequency $2\sqrt{n}\Omega$. The population $P_n(t)$ is then obtained by the Fourier transformation of $P_e(\tau')$,

$$\begin{aligned}\tilde{P}_e(\omega') &= \frac{1}{T}\int_0^T d\tau' P_e(\tau')\cos\omega'\tau' \\ &= \frac{1}{2}\sum_n P_n(t)\left[\frac{1}{2}\frac{\sin(2\sqrt{n}\Omega+\omega')T}{(2\sqrt{n}\Omega+\omega')T}\right. \\ &\quad \left.+\frac{1}{2}\frac{\sin(2\sqrt{n}\Omega-\omega')T}{(2\sqrt{n}\Omega-\omega')T}+\frac{\sin\omega' T}{\omega' T}\right],\end{aligned} \tag{44}$$

where T denotes the measuring time. Equation (44) is composed of the functions $\sin[(x-a)T]/(x-a)T$. These functions have a peak with height of 1 and width of $2\pi/T$ at $x=a$. Therefore, the first and second terms in Eq. (44) have peaks at $\omega' = \pm 2\Omega\sqrt{n}$ with a height of $P_n(t)/4$. The third term has a peak with a height of $P_0(t)/2$ at $\omega' = 0$. Therefore, the population probability $P_n(t)$ is measured from the height of each peak.

Note that there is a lower bound for the measuring time used to distinguish each peak because the distance between adjacent peaks $2\Omega(\sqrt{n+1}-\sqrt{n})$ becomes increasingly narrow at higher energy levels and each peak has a finite width of $2\pi/T$. Thus the nth peak overlaps the adjacent $(n+1)$th peak when $2\pi/T > 2\Omega(\sqrt{n+1}-\sqrt{n})$. Thus, the lower bound for the measuring time is

$$T > \frac{\pi}{\Omega(\sqrt{n+1}-\sqrt{n})}. \tag{45}$$

A longer measuring time is required for detecting higher energy peaks, for example, $\Omega T > 20$ for $n = 10$.

Decoherence in the coherent motion of probability densities between the qubit and the double SQUID modifies the above relations. We phenomenologically introduce dissipation by replacing Eq. (43) with $P_e(\tau')e^{-\gamma\tau'}$ with γ being the phenomenological decay rate. The Fourier spectrum of $P_e(\tau')e^{-\gamma\tau'}$ is given as

$$\begin{aligned}\tilde{P}_e(\omega',\gamma) = \frac{1}{2}e^{-\gamma T}\sum_n P_n(t) \\ \times\Bigg(&\frac{1}{2\{[2\sqrt{n}\Omega T+(\omega' T)]^2+(\gamma T)^2\}} \\ &\times\{[2\sqrt{n}\Omega T+(\omega' T)]\sin[2\sqrt{n}\Omega T+(\omega' T)] \\ &-(\gamma T)\cos[2\sqrt{n}\Omega T+(\omega' T)]+(\gamma T)e^{\gamma T}\} \\ &+\frac{1}{2\{[2\sqrt{n}\Omega T-(\omega' T)]^2+(\gamma T)^2\}} \\ &\times\{[2\sqrt{n}\Omega T-(\omega' T)]\sin[2\sqrt{n}\Omega T-(\omega' T)] \\ &-(\gamma T)\cos[2\sqrt{n}\Omega T+(\omega' T)]+(\gamma T)e^{\gamma T}\} \\ &+\frac{(\omega' T)\sin\omega' T-(\gamma T)\cos\omega' T+(\gamma T)e^{\gamma T}}{(\omega' T)^2+(\gamma T)^2}\Bigg).\end{aligned} \tag{46}$$

In general, dissipation broadens the peak width associated with the term

$$\frac{e^{-\gamma T}(x\sin x-\gamma T\cos x)+\gamma T}{x^2+(\gamma T)^2}, \tag{47}$$

indicating a peak at $x=0$ with height $(1-e^{-\gamma T})/\gamma T$. The peak width is determined by

$$e^{-\gamma T}(x\sin x-\gamma T\cos x)+\gamma T = 0. \tag{48}$$

With weak dissipation $\gamma T \simeq 0$, the deviation δ from the nondissipative width π is expected to be small. In fact, Eq. (48) is reduced to

$$-\pi\delta+\gamma T+\gamma T e^{\gamma T} = 0.$$

The extra broadening due to dissipation is then $\delta \simeq \gamma T(1+e^{\gamma T})/\pi$. The deviation δ is $0.22 \ll \pi$ when $1/\gamma = 2.5\ \mu$s[32] and $T = 1.25\ \mu$s, i.e., $\gamma T = 0.3$. Therefore, Eq. (45) is still applicable with weak dissipation. On the other hand, the measuring time T should be much shorter than the decoherence time $1/\gamma$ because the peak height is suppressed by the factor $e^{-\gamma T}$. This determines the upper bound of the measuring time.

By taking account of the upper and lower bounds Eq. (45), the measuring time for the nth level with dissipation is given as

$$\frac{1}{\gamma} \gg T > \left(\frac{\pi}{\Omega}\right)\frac{1}{\sqrt{n+1}-\sqrt{n}}. \tag{49}$$

From this restriction, the measuring time T should be $2.5\mu\text{s} \gg T > 0.5\mu\text{s}$ with the current experimental parameters. Figure 6 shows the Fourier spectrum for Rabi oscillations between a qubit and a double SQUID. The dotted and solid lines in Fig. 6 denote the Fourier spectrum without dissipation ($\gamma = 0$) and with dissipation $\gamma/\Omega = 1/(2.5\mu\text{s}\times 0.04\,\text{GHz}) = 0.01$, respectively. Even with dissipation, significant distribution properties such as even-numbered occupation can be clearly found from the spectrum.

Note that the dynamical Casimir effect is the amplification of the quantum fluctuation in the ground state due to the nonadiabatic boundary effect. Thus, to remove any form of uncontrollable noise sources, including thermal noises that are naturally occurring in the proposed design circuit, a low-noise amplifier[33] and/or low temperature systems should be required. Therefore, a quantum-circuit analog of the dynamical Casimir effect can be established in a double SQUID by detecting the super-Poissonian distribution peculiar to squeezing that originates from the nonadiabatic boundary effect.

Finally, it is worth mentioning the direct observation of squeezing in detecting the reduced fluctuation of one of conjugate observables, i.e., magnetic flux Φ threading in the large loop of our double SQUID system, by homodyne detection scheme. The fluctuation $\Delta\Phi$ is roughly estimated as $\Delta\Phi = \exp[-|\mu|]\Delta\Phi_0 = 0.42\Delta\Phi_0$ when the squeezing parameter $|\mu|$ is 0.87 given by single-step frequency modulation from $\omega_0 = 59$ (GHz) to $\omega_1 = 10$ (GHz). Here $\Delta\Phi_0$ denotes the ground-state flux fluctuation, typically

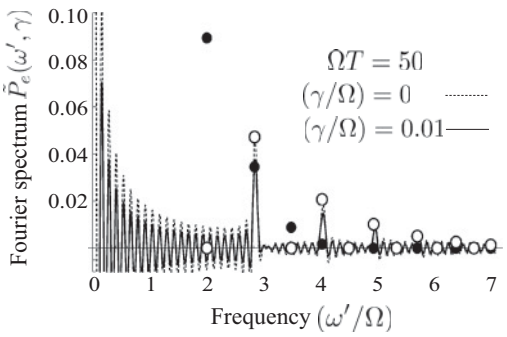

FIG. 6. Fourier spectra of $\tilde{P}_e(\tau')$ with the dissipation given by Eq. (46). The solid and dotted lines denote the Fourier spectrum with dissipation ($\gamma/\Omega = 0.01$) and without dissipation ($\gamma/\Omega = 0$), respectively. The white circles denote the population distribution $P_n(t)/4$ for squeezing parameter $|\nu(t)| = 1$. For comparison, the distribution of the coherent state with same average photon number is denoted by the black circles. The odd-numbered excitations peculiar to squeezed states enable us to identify the dynamical Casimir effect.

$\Delta\Phi_0 = 7.8 \times 10^{-18}$ (Wb) in our junction parameter $C =$ 15 (pF). All these can be made possible with the use of the innovative technology. Further details will be discussed in later articles.

VI. CONCLUSION

We have investigated the nonstationary properties of a quantum flux in a double SQUID system regarded as an analog of an electrically neutral cavity with a moving boundary in a vacuum. We have formulated quantum-state evolutions of the double SQUID states based on the Bogoliubov transformation between eigenstates at different times. As a result, squeezed states of the quantum flux in the double SQUID are produced as a result of the nonadiabatic effect. The analytic formula, Eq. (21), and numerical results show that the squeezing parameter can measure the nonstationary aspect of the quantum flux in the double SQUID. In addition, the super-Poissonian distribution peculiar to squeezing with a significant characteristic such as an even-numbered population is superior to conventional single-photon detection techniques in terms of measuring nonadiabatic effects. We have demonstrated that both sudden and sinusoidal frequency modulations produce sufficiently strong nonadiabatic effects. Thus, a nonstationary boundary effect can be implemented in a circuit QED system. In other words, Josephson quantum circuits are suitable for exploring the dynamical properties of quantum systems due to the high quantum coherence and rapid controllability with low dissipation.

In addition, we showed that the dynamical effect can be formulated with a Hamiltonian similar to the interaction Hamiltonian of photons with a nonlinear optical crystal in quantum optics. The analogy of the Hamiltonians of the two systems suggests that a double SQUID behaving like a time-dependent harmonic oscillator can be regarded as a nonlinear optical material with a tunable nonlinear optical susceptibility. The nonlinear property is used to provide a coupler between the quantum bits[34,35] in quantum information technology. Controllable susceptibility is a preferable characteristic for couplers in quantum information technology. Therefore, the present results indicate that the double SQUID has the potential for quantum information applications.

ACKNOWLEDGMENTS

We are grateful to A. Ustinov, S. Poletto, M. Nishida, and S. Kawabata for valuable discussions. One of the authors (T.F.) is grateful to S. Tanda and T. Honma for their continuous encouragement. This work was supported in part by a grant from the Research Foundation for Opto-Science and Technology and Special Postdoctoral Researcher of Hiroshima University.

*Current address: Department of Physics, Asahikawa Medical University, Midorigaoka-higashi, Asahikawa 078-8510, Japan, Research Institute for Science and Engineering, Waseda University, Shinjuku-ku, Tokyo 169-8555, Japan.

[1] H. B. G. Casimir, Proc. K. Ned. Akad. Wet. **51**, 793 (1948).
[2] S. K. Lamoreaux, Phys. Rev. Lett. **78**, 5 (1997).
[3] U. Mohideen and A. Roy, Phys. Rev. Lett. **81**, 4549 (1998).
[4] G. T. Moore, J. Math. Phys. **11**, 2679 (1970).
[5] E. Yablonovitch, J. P. Heritage, D. E. Aspnes, and Y. Yafet, Phys. Rev. Lett. **63**, 976 (1989).
[6] H. Saito and H. Hyuga, Phys. Rev. A **78**, 033605 (2008).
[7] N. M. Lawandy, Opt. Lett. **31**, 3650 (2006).
[8] J. R. Johansson, G. Johansson, C. M. Wilson, and F. Nori, Phys. Rev. Lett. **103**, 147003 (2009).
[9] E. Segev, B. Abdo, O. Shtempluck E. Buks, and B. Yurke, Phys. Lett. A **370**, 202 (2007).
[10] V. V. Dodonov, V. I. Man'ko, and O. V. Man'ko, J. Sov. Laser Res. **10**, 413 (1989).
[11] V. V. Dodonov, A. B. Klimov, and V. I. Man'ko, Phys. Lett. A **142**, 511 (1989).
[12] V. I. Man'ko, J. Sov. Laser Res. **12**, 383 (1991).
[13] O. V. Man'ko, J. Korean Phys. Soc. **27**, 1 (1994).
[14] V. V. Dodonov, Adv. Chem. Phys. **119**, 309 (2001).
[15] K. Hushimi, Prog. Theor. Phys. **9**, 381 (1953).
[16] W. H. Louisell, A. Yariv, and A. E. Siegman, Phys. Rev. **124**, 1646 (1961).
[17] M. Hotta, I. Joichi, Sh. Matsumoto, and M. Yoshimura, Phys. Rev. D **55**, 4614 (1997).
[18] V. V. Dodonov, V. I. Man'ko, and O. V. Man'ko, J. Sov. Laser Res. **10**, 413 (1989).
[19] A. M. Perelomov and B. Y. Zel'dovich, *Quantum Mechanics: Selected Topics* (World Scientific, Singapore, 1999).
[20] K. K. Likharev and V. K. Semenov, IEEE Trans. Appl. Supercond. **1**, 3 (1991).
[21] K. Takashima, N. Hatakenaka, S. Kurihara, and A. Zeilinger, J. Phys. A **41**, 164036 (2008).
[22] K. Takashima, S. Matsuo, T. Fujii, N. Hatakenaka, S. Kurihara, and A. Zeilinger, J. Phys.: Conf. Ser. **150**, 052260 (2009).
[23] S. Han, J. Lapointe, and J. E. Lukens, Phys. Rev. Lett. **63**, 1712 (1989).
[24] S. Han, J. Lapointe, and J. E. Lukens, Phys. Rev. B **46**, 6338 (1992).
[25] M. G. Castellano, F. Chiarello1, P. Carelli, C. Cosmelli, F. Mattioli, and G. Torrioli, New J. Phys. **12**, 043047 (2010).
[26] H. P. Yuen, Phys. Rev. A **13**, 2226 (1976).
[27] V. V. Dodonov and A. V. Dodonov, J. Russ. Laser Res. **26**, 445 (2005).
[28] R. Adam, M. Currie, C. Williams, R. Sobolewski, O. Harnack, and M. Darula, Appl. Phys. Lett. **76**, 469 (2000).
[29] D. I. Schuster *et al.*, Nature **445**, 515 (2007).
[30] M. Hofheinz *et al.*, Nature **454**, 310 (2008).
[31] T. P. Orlando, J. E. Mooij, L. Tian, C. H. van der Wal, L. Levitov, S. Lloyd, and J. J. Mazo, Phys. Rev. B **60**, 15398 (1999).
[32] A. Y. Smirnov, Phys. Rev. B **68**, 134514 (2003).
[33] S. Intiso, J. Pekola, A. Savin, Y. Devyatov, and A. Kidiyarova-Shevchenko, Supercond. Sci. Technol. **19**, S335 (2006).
[34] Y. Yamamoto, M. Kitagawa, and K. Igeta, in *Proceedings of the 3rd Asia-Pacific Physics Conference* (World Scientific, Singapore, 1988).
[35] G. J. Milburn, Phys. Rev. Lett. **62**, 2124 (1989).